FDD method for a variable-speed heat pump with natural refrigerants

Ivan Bellanco [a,b], *Francisco* Belío [a], *Manel* Vàlles [b], *Raphael* Gerber [c], *Jaume* Salom [a]

[a] Catalonia Institute for Energy Research (IREC), Jardins de les Dones de Negre 1, Sant Adrià del Besòs (Barcelona), 08930, Spain. ibellanco@irec.cat, jfbelio@irec.cat, jsalom@irec.cat

[b] Department of Mechanical Engineering, Unirversitat Rovira i Virgili, Av. Països Catalans No. 26, Tarragona, 43007, Spain. manel.valles@urv.cat

[c] Heim AG Heizsysteme, Wittenwilerstrasse 31, Aadorf, 8355, Switzerland. Raphael.Gerber@heim-ag.ch

Abstract. Heat pumps are one of the most efficient devices to provide heat and cool. The number of heat pumps sold in Europe increases every year as European Legislation moves towards the use of natural refrigerants that have negligible global warming potential compared to synthetic refrigerants. Variable-speed domestic heat pumps may have hard-to-detect faults that increase energy consumption while the demand is still covered. These faults could worsen and take down the equipment. Fault detection and diagnosis (FDD) systems aim to detect these types of soft faults, reducing operating and maintenance costs. The present study is the result of developing an FDD system for variable-speed heat pumps. The FDD system has been tested with a 10 kW water-to-water variable-speed heat pump charged with propane. Some of the most common faults were emulated for 10 kW and 12 kW heating loads. These faults were evaporator fouling, compressor valve leakage, liquid line restriction and refrigerant overcharge. The present paper presents the overall structure of the developed FDD, each of its different modules and the performance indicators during tests. The FDD developed consists of different modules: a steady-state detector, the input space module, the no-fault regression models and the diagnosis module. The steady-state detector filters the measurements to select only the steady-state data. The input space classifies the data in clusters defined by the heat pump driving variables. For each of these clusters, a regression model is trained. Once trained, the deviation between the models and the real data will indicate a fault occurrence. The diagnosis module analyses the trends of different features to diagnose the fault. The FDD was able to monitor in real time the heat pump performance during the fault tests. The results showed fault detection before 10 minutes with COP drifts above 7 %. Each fault could be diagnosed correctly, except evaporator fouling, which was detected as a fault but could not be distinguished from the others.

Keywords. FDD, variable speed heat pump, natural refrigerants
DOI: https://doi.org/10.34641/clima.2022.433

1. Introduction

In the European Union, a large part of the energy consumption in households is due to space heating, water heating and space cooling [1]. Heat pumps are one of the most efficient technologies for space heating and cooling and, coupled with renewable electricity sources they can reduce greenhouse emissions compared with classic solutions. However, the refrigerants used in heat pumps could have high global warming potential (GWP). These refrigerants could leak to the environment due to a leakage in the circuit or incorrect disposal at the end of life. For this reason, the restrictions to the use of refrigerants with high GWP are increasing, promoting the use of natural refrigerants, such as propane or carbon dioxide with lower GWP.

Despite their high performance, heat pumps could suffer fault conditions that can affect their optimal operation and reduce their energy efficiency [2]. There is a typology of faults called “soft faults” because they reduce the equipment efficiency while still covering the demand, making them difficult to detect [3]. These faults could remain undetected for long periods, increasing the energy consumption and could worsen and damage the heat pump. Fault Detection and Diagnosis (FDD) systems are used to detect soft faults or performance decreases [4].

Generally, the structure of an FDD is as follows: a learning phase where a model of the normal

operation of the heat pump is generated. The model could be trained with simulation, manufacturer or experimental data. Once trained, the measurements from the heat pump are compared with those coming from the models. If there is a difference, a fault is occurring. The diagnosis is usually performed by checking the trends of different features of the heat pump. Depending on the feature and if its trend is increasing or decreasing, the FDD could diagnose the fault. Machine learning could be used to avoid the need for expert knowledge about the fault effect, but it requires fault data to train the algorithms [5].
The present study describes the experimental evaluation of a new developed FDD. The general scheme of the FDD is explained and each part is described. A variable-speed heat pump charged with propane is used to emulate different faults. The tests data are used to train and validate the FDD algorithm.

2. Methodology

For this study, two different heating load conditions at steady state were tested, 10.2 kW and 12.3 kW. Table 1 shows the temperatures and water flows of the circuits for those conditions. The water flow was fixed. First, the heat pump with no fault was tested at those two conditions. Then, the faults evaporator fouling (EF), compressor valve leakage (CVL), liquid line restriction (LL) and refrigerant overcharge (OC) were tested for both conditions.

Tab. 1 – Steady-state test conditions. From the water side: condenser outlet temperature ($T_{cond,out}$), condenser inlet temperature ($T_{cond,in}$), evaporator inlet temperature ($T_{evap,in}$), condenser water flow ($\dot{V}_{cond}$) and evaporator water flow ($\dot{V}_{evap}$).

Heating load	$T_{cond,out}$	$T_{cond,in}$	$T_{evap,in}$	$\dot{V}_{cond}$	$\dot{V}_{evap}$
(kW)	(ºC)	(ºC)	(ºC)	(lpm)	(lpm)
10.2	45	40	10	30	40
12.3	45	40	10	30	40

2.1 Evaporator fouling

In air heat pumps, the evaporator is normally located outdoors, where it is exposed to dirt and particles that can obstruct the heat exchanger. In water heat pumps, dirt could accumulate in the impeller of the pump [6]. In both heat pump typologies, mechanical faults as pump or fan malfunction can also appear. All these faults decrease the heat transfer coefficient and have been grouped in this paper under the term "Evaporator fouling". To emulate the fault, the water flow of the evaporator was decreased below the nominal value. Equation 1 describes the fault intensity (FI) related to this water flow decrease.

$$FI_{EF} = \frac{\dot{V}_{fault} - \dot{V}_{nom}}{\dot{V}_{nom}} \quad (1)$$

where $\dot{V}_{fault}$ is the evaporator water flow for the current fault level and $\dot{V}_{nom}$ is the water flow for the no-fault condition. The nominal water flow was 40 lpm.

2.2 Compressor valve leakage

The compressor valve leakage refers to a bypass between the high and low-pressure sides of the refrigerant circuit. This leakage could appear in the compressor or in the 4-way valves [6]. The fault was emulated by opening a valve that bypasses the discharge and suction sides of the compressor. Equation 2 describes the fault intensity related to the refrigerant mass flow.

$$FI_{CVL} = \frac{\dot{m}_{r\_fault} - \dot{m}_{r\_nom}}{\dot{m}_{r\_nom}} \quad (2)$$

where $\dot{m}_{r\_fault}$ is the refrigerant mass flow for the fault condition and $\dot{m}_{r\_nom}$ is the refrigerant mass flow when no fault is present. As $\dot{m}_{r\_nom}$ changes with the speed of the compressor, a correlation between speed and flow was obtained running the compressor at different speeds when no fault is present.

2.3 Liquid line restriction

The liquid line restriction appears when the filter placed in the liquid line gets fouled by debris in the refrigerant. This fouling increases the pressure drop of the liquid line [6]. The fault was emulated with a restriction valve placed in the liquid line. Equation 3 shows the fault intensity for this fault, which is related to the pressure drop variation in the liquid line.

$$FI_{LL} = \frac{\Delta P_{LL} - \Delta P_{nom}}{\Delta P_{nom}} \quad (3)$$

where ΔP_{LL} represents the liquid line pressure drop with fault and ΔP_{nom} the liquid line pressure drop without fault. The pressure drop was calculated as the difference between discharge and suction pressures.

2.4 Refrigerant overcharge

An overcharge of refrigerant occurs when more refrigerant than the nominal amount is charged during a commissioning or maintenance service [6]. The fault was emulated charging a 10% more refrigerant than the nominal. Equation 4 shows the fault intensity for OC.

$$FI_{OC} = \frac{m_{r\_fault} - m_{r\_nom}}{m_{r\_nom}} \quad (4)$$

2.5 Equipment and validation procedure

A 10 kW variable-speed water-to-water heat pump was tested. The heat pump was a prototype developed in the framework of the *Trigeneration systems based on heat pumps with natural refrigerants and multiple renewable sources* (TRI-HP

project) [7] charged with 720 grams of propane as refrigerant. Figure 1 shows the heat pump scheme. More information about the heat pump architecture, the experimental procedure and the fault test results can be found in [8]. The no-fault data was used to train the FDD and the fault data was used to validate the FDD performance.

3. Fault detection and diagnosis algorithm

Despite the use of two steady state conditions, the development of the FDD algorithm has been focused on the use of different heat pumps at different conditions. Because of that, the algorithm counts with different modules to increase the detection accuracy. These modules are a steady state detector, an input space classifier, the regression model training and fault monitoring, and fault diagnosis. Figure 2 shows the operation flow scheme of the FDD.

3.1 Steady state detector

The objective of the steady-state detector (SSD) is to identify the stages where the heat pump is working at quasi-steady-state conditions to use the data for training and fault monitoring [9]. In statistics, a data series is in steady state when the slope of the mean and the variance is constant and there is no seasonality. When real-time data is used, sensor noise and variability due to variable speed operation will lead to a non-constant value of the mean and variance. Because of this, the detector will search for points with quasi-stationarity, where a percentage of change in variance and mean is allowed. A sliding window method [9] is applied for the calculation of the mean and variance slope. The mean and variance of the first window are used as a reference. Then, it is compared to the adjacent windows. If the mean and variance of all the windows are in inside the threshold then, the last point will be in steady state. The threshold was determined from an average of experimental data of previous tests with variable and fixed speed heat pumps

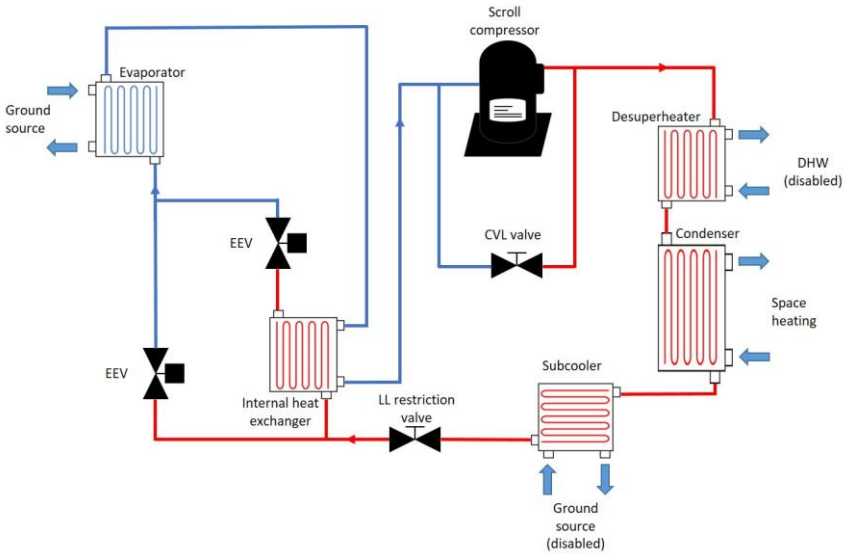

Fig. 1 – Heat pump architecture. The desuperheater and subcooler were not used during the tests.

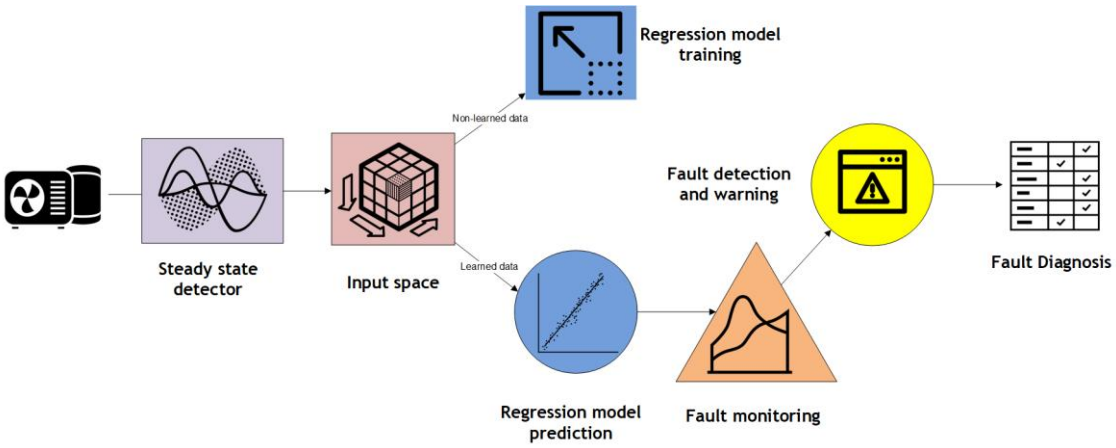

Fig. 2 – Software scheme of the FDD.

3.2 Input space classifier

Most of the FDD are developed to work under steady state conditions where the conditions do not change. Based on the work of Heo et al. [10], we used an input space classifier to allow the training of new data. The input space is the three-dimensional area defined by the independent or driving variables of the heat pump [11]. For a variable-speed heat pump, we choose the condenser outlet and inlet temperatures ($T_{cond,out}$ $T_{cond,in}$) and the evaporator inlet temperature ($T_{evap,in}$) as the driving variables. Figure 3 shows a representation of the input space division in groups. For each of these groups, a no-fault model could be trained.

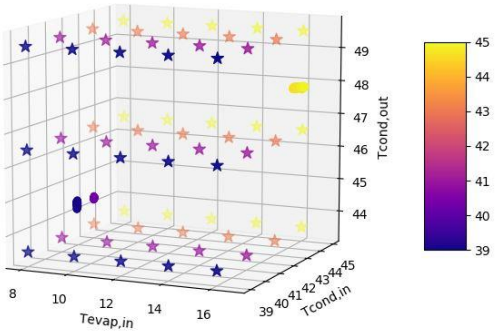

Fig. 3 – Input Space. The stars are the arithmetic center of each group. The points are the training data. The color scale is used in the $T_{cond,in}$ axis.

3.3 Regression model training and fault monitoring

For the generation of no-fault models, a stochastic gradient descent regression approach was selected for its good results and low requirement of computational power. During a defined period, while there is no fault present, the measurement data is stored. Once the period is over, the input space classifies the data into groups, and if there are enough data points (at least 50), a model will be trained for each group. This is the initial training period. When the current driving conditions are beyond those of the training period, the algorithm will store the data until there are enough data points to train that group. This gives the capability of self-training the algorithm.

After the initial training period, the data coming from the heat pump will be compared with the corresponding no-fault model. An uncertainty margin is applied to the original prediction of the FDD. This area is two times the maximum root-mean-square error (RMSE) of the cluster training. Figure 4 shows the uncertainty margin of a model of one of the clusters of the input space. If the coefficient of performance (COP) of the heat pump is outside this margin a fault could be happening. However, noise or outliers in the measurement could be outside this margin without an actual fault happening. Because of that, when there is a drift between the COP of the model and the COP measured, the algorithm starts a counter. A warning flag will be triggered if, for a period of ten minutes, the number of measurements outside the uncertainty margin represents more than 80% of the samples. Figure 5 shows an example of fault monitoring with a 30 minutes counter.

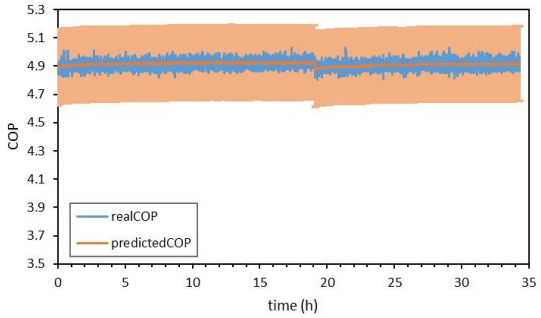

Fig. 4 – Training results of an Input Space cluster. The blue line is the real data. The orange one is the prediction of the algorithm. The shadowed area is the uncertainty margin.

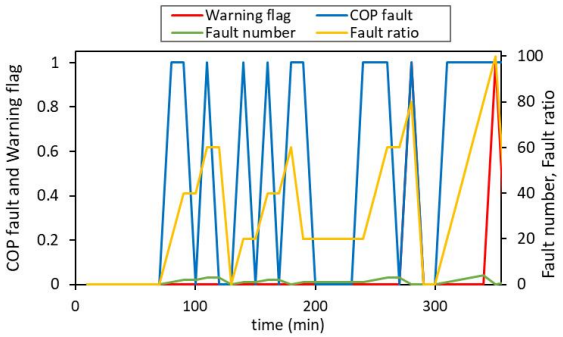

Fig. 5 – Fault monitoring example from a series with 10 minute frequency and 50 minutes of monitoring. COP flag is triggered when the COP measurements are outside the uncertainty range. Fault ratio is the percentage of measurements outside the uncertainty in the monitoring window. The warning flag is triggered when the fault ratio is above 80%.

3.4 Fault diagnosis

Once a fault warning is triggered, the algorithm will look at different trends of the heat pump features to diagnose the fault. In our case, we consider as valuable features the COP, the compressor electrical consumption (W_{comp}), the heat duty (Q_{heat}), the subcooling (T_{sc}), the superheating (T_{sh}), the evaporation temperature (T_{evap}), the condenser temperature (T_{cond}), the compressor outlet temperature (T_{co}), the liquid line refrigerant temperature (T_{ll}), the refrigerant mass flow (m_r) and the compressor frequency (f). For each of these features, a no-fault model is trained. The actual value is compared with the one from the models and three different trends are considered: increasing, decreasing or no change. The result is compared with a trend chart that serves to diagnose the fault.

Tab. 6 – Trend chart used to diagnose faults. ↓: decreasing trend, ↑: increasing trend.

Fault	COP	W_{comp}	Q_{heat}	T_{sc}	T_{sh}	T_{evap}	T_{cond}	T_{co}	T_{ll}	m_r	f
EF	↓	↑				↓					↑
CVL	↓	↑	↓	↑				↑	↓	↓	↑
LL	↓	↑		↑	↑	↓	↑	↑	↓	↓	↑
OC	↓	↑		↑		↑	↑	↑	↓		↓

Tab. 7 – Performance values for the FDD. "-": When the FDD did not reach any detection.

Code	FI	Accuracy (%)	COP drift (%)	Code	FI	Accuracy (%)	COP drift (%)
EF10.1	-0.100	-	0	CVL10.1	-0.042	-	2
EF10.2	-0.157	-	0	CVL10.2	-0.296	100	22
EF10.3	-0.214	-	1	CVL10.3	-0.372	100	29
EF10.4	-0.271	-	1	CVL10.4	-0.648	-	21
EF10.5	-0.328	-	2	CVL12.1	-0.131	100	11
EF10.6	-0.385	100	3	CVL12.2	-0.379	100	31
EF10.7	-0.442	100	4	CVL12.3	-0.608	100	47
EF10.8	-0.500	100	5	LL10.1	0.103	100	7
EF12.1	-0.100	-	1	LL10.2	0.181	100	14
EF12.2	-0.157	-	1	LL10.3	0.267	100	18
EF12.3	-0.214	-	2	LL10.4	0.418	100	26
EF12.4	-0.271	-	3	LL10.5	0.743	100	35
EF12.5	-0.328	-	3	LL12.1	0.055	-	2
EF12.6	-0.385	-	4	LL12.2	0.168	100	13
EF12.7	-0.442	-	6	LL12.3	0.281	100	19
EF12.8	-0.500	100	7	LL12.4	0.404	100	24
OC10.1	0.100	100	21	LL12.5	0.648	100	31
OC10.2	0.100	100	19				

4. Results and discussion

Table 6 summarizes the feature trends obtained in the fault tests [8]. This table serves to diagnose faults based on the trends of the different features. To evaluate the performance of the FDD, the indicators accuracy and COP drift were used.

The accuracy represents the fraction of correct fault warnings with respect to the total fault warnings given by the FDD system.

$$Accuracy = \frac{True\ \text{Positive}}{True\ Positive + False\ positive} \quad (5)$$

Equation 5 shows the Accuracy equation where a true positive means that the FDD detects a fault when it is actually happening and false positive when the FDD detects a fault when there is none.

The COP drift indicates the degree of COP deterioration as equation 6 shows. An ideal FDD should have a 100% accuracy and detect from 1% of COP drift.

$$COP\ drift = \frac{COP_{nominal} - COP_{fault}}{COP_{nominal}} * 100 \quad (6)$$

Table 7 shows the performance values for each fault level tested. The FDD detected COP drifts above 3% and 7%. A 100% accuracy was obtained when the FDD detected a fault. This means that the FDD did not give any false alarms. Figure 4 shows the training results of an input space cluster. Despite the use of an SSD, the uncertainty area is remarkable. The use of such a margin was to eliminate the possibility of false alarms and increase the reliability of the algorithm. The margin could be narrowed so the FDD could detect lower COP drifts in exchange for a higher probability of false alarms.

Table 8 shows the diagnosis results of the FDD. The indicator Misdiagnosis Rate (MR) was used to indicate the capability of the FDD for correctly

diagnose the faults detected. Equation 7 shows the calculation of MR, which is related to the number of incorrect diagnoses provided by the FDD.

$$MR = \frac{False\ Diagnosis}{False\ Diagnosis+True\ Diagnosis} \quad (7)$$

Except for EF, all the faults could be correctly diagnosed. EF had the lowest impact on the heat pump, which is the reason for not reaching a diagnosis. Nevertheless, the algorithm detects that there is a fault but cannot discern which.

Tab. 8 – MR values for the diagnosis module. "-": the algorithm does not reach a diagnose.

Code	MR (%)
EF10	-
EF12	-
CVL10	0
CVL12	0
LL10	0
LL12	0
OC10	0
OC12	0

5. Conclusions

A new FDD developed for variable-speed heat pumps has been validated with real equipment data. To do so, some of the most common faults on heat pumps has been emulated in a variable-speed heat pump charged with propane. The FDD is composed of different modules to ensure the efficiency of the algorithm. The use of an SSD and a fault monitoring module increases the accuracy of the algorithm and reduces the number of false alarms. However, this increases the time needed to detect a fault (less than 30 minutes). The use of regressions decreases the computational power needed to monitor the equipment and limits the training data needed. The self-training capability has not been needed for the experimental tests, as the same conditions were used for training and monitoring. But the use of self-training could be risky. The heat pump is considered with no fault when it has been installed and commissioned by a certified technician. After that, if the algorithm self-trains, it could do it when there is a fault on the equipment. The use of manufacturer data could help to tackle the problem, but more research is needed in this aspect.
With COP losses of as much as 47%, the use of FDD takes more relevance as the faults tested have not decreased the heat provided by the heat pump and therefore, the user does not detect the problem.

6. Acknowledgement

Ivan Bellanco acknowledges the Universities and Research Secretariat of the Catalan Government and the European Social Fund for the financial support of the predoctoral contract 2019FI_B 00928.

The research conducted in this paper is partially funded by the European Union's Horizon 2020 research and innovation program under grant agreement No.814888 (TRI-HP).

7. References

[1]Eurostat Statistic Explained. Energy consumption in households [Internet]. Online. 2019 [cited 2021 Dec 13]. Available from: https://ec.europa.eu/research/foresight/index.cfm

[2]Domanski P.A., Henderson H.I., Payne W.V., Domanski P.A., Henderson H.I., Payne W.V. Sensitivity Analysis of Installation Faults on Heat Pump Performance. NIST Technical Note 1848. 2014.

[3]Janecke A., Terrill T.J., Rasmussen B.P. A comparison of static and dynamic fault detection techniques for transcritical refrigeration. Int J Refrig [Internet]. 2017;80:212–24. Available from: http://dx.doi.org/10.1016/j.ijrefrig.2017.04.020

[4]Katipamula S., Brambley M.R. Review article: Methods for fault detection, diagnostics, and prognostics for building systems—a review, part I. HVAC R Res. 2005;11(1).

[5]Rogers A.P., Guo F., Rasmussen B.P. A review of fault detection and diagnosis methods for residential air conditioning systems. Build Environ [Internet]. 2019;161(July):106236. Available from: https://doi.org/10.1016/j.buildenv.2019.106236

[6]Bellanco I., Fuentes E., Vallès M., Salom J. A review of the fault behavior of heat pumps and measurements, detection and diagnosis methods including virtual sensors. J Build Eng. 2021;39(August 2020).

[7]TRI-HP project: Trigeneration systems based on heat pumps with natural refrigerants and multiple renewable sources [Internet]. [cited 2022 Jan 11]. Available from: https://www.tri-hp.eu/

[8]Bellanco I., Belío F., Vallés M., Gerber R., Salom J. Common fault effects on a natural refrigerant, variable-speed heat pump. Int J Refrig. 2022;133(January 2022):259–66.

[9]Kim M., Yoon S.H., Domanski P.A., Vance Payne W. Design of a steady-state detector for fault detection and diagnosis of a residential air conditioner. Int J Refrig. 2008;

[10]Heo J., Payne W.V., Domanski P.A., Du Z. Self Training of a Fault-Free Model for Residential Air Conditioner Fault Detection and Diagnostics. 2015.

[11]Kim M., Yoon S.H., Payne W.V., Domanski P.A. Development of the reference model for a residential heat pump system for cooling mode fault detection and diagnosis. J Mech Sci Technol. 2010;24(7):1481–9.

Data Statement

The data from the fault tests is accessible through the dataset Ivan Bellanco, Francisco Belío, Raphael Gerber, & Jaume Salom. (2021). Common faults tested on a variable-speed propane-charged heat pump on heating mode (Version 1). Zenodo. https://doi.org/10.5281/zenodo.5155136